Cartographic scripts for seismic and geophysical mapping of Ecuador

POLINA LEMENKOVA

Université libre de Bruxelles, École polytechnique de Bruxelles, Laboratory of Image Synthesis and Analysis, Brussels, Belgium; e-mail: polina.lemenkova@ulb.be, pauline.lemenkova@gmail.com

ABSTRACT This research describes a script-based method of Generic Mapping Tools (GMT) for mapping the seismicity, geophysics, geology and topography of Ecuador. The advances of GMT include the following points: (1) automation of workflow; (2) refined aesthetics of graphics; (3) speed console-based mapping; (4) multi-format data handling; (5) advanced syntax. An explanation of scripting with the examples of code snippets is provided. The results present six new maps of Ecuador. The distribution of geophysical phenomena and seismicity is compared to the terrain elevation, showing remarkable correlations with the topography and geoid. The data demonstrated low values in the depression of the Andes, the Gulf of Guayaquil, and the Peru-Chile Trench. The peaks in gravity are representative for the Andean topography. Local decreases in gravity correspond to the depressions in the coastal shelf and the Gulf of Guayaquil. The increase in seismicity is detected along the tectonically active areas. The GMT is appropriate to the geological risk assessment of Ecuador.

KEY WORDS seismicity – geophysics – GMT – Earth observation – cartography

LEMENKOVA, P. (2022): Cartographic scripts for seismic and geophysical mapping of Ecuador. Geografie, 127, 3, 195–218.
https://doi.org/10.37040/geografie.2022.006
Received November 2021, accepted May 2022.

1. Introduction

For seismically active regions, such as the South American Andes, spatial variations in the earthquakes are studied through the variety of geophysical methods. The approaches of risk assessment and seismic hazard monitoring consist of mapping and modelling earthquakes. Important actions include the analysis of seismic parameterse.g., earthquake sources, focal mechanisms, depth, magnitude, repeatability, rupture velocity, generation of tsunami and volcanism (Agurto-Detzel et al. 2019; Jiménez, Saavedra, Moreno 2021; Legrand et al. 2002; Yamanaka, Tanioka, 2018). Other methods include detecting seismo-ionospheric anomalies in the epicenters (Akhoondzadeh et al. 2018), geodynamical data mapping (Font et al. 2013; Álvarez, Folguera, Gimenez 2017; Lemenkova, 2019a, 2020a), geodetic observations of seismic episodes, interactions between the earthquakes and volcanoes using remote sensing radar data (Ebmeier et al. 2016).

The importance of monitoring earthquakes is caused by their direct consequences on nature and man. These include affecting and changingnatural landscapesby landslides, mass Displacements as mentioned in geophysical studies (Sevilla 1992, Schuster et al. 1996, Lemenkova 2021e). Negative social consequences include damaged property or losses of human lives, as a result of the earthquakes (Cevallos-Merki, Joerin 2021). Due to the location in the tectonically active region of Andes and complex geological setting, Ecuador is exposed to a high risk of seismic hazards from the tectonic plate subduction as a result of the colliding Nazca/South America plates in northern Ecuador (Vaca et al. 2018). In turn, the tectonic activity causes repetitive moderate to large shallow crustal earthquakes (Beauval et al. 2018). The Instituto Geofísico of the Escuela Politécnica Nacional (IGEPN) of Ecuador performs regular and accurate seismic observations and monitoring of the country at national level. Currently, earthquake monitoring in Ecuador is based on seismic, volcanic, and geodetic networks with 81 seismic stations, 117 strong-motion sensors, 85 Global Positioning System (GPS) stations, and 8 first and second level volcano observatories (at least 2 independent monitoring techniques). These institutes supply the information regarding seismicity at the national seismic and volcanic data center, which maintains raw and processed seismic, volcanic, and geodetic data (Alvarado et al. 2018).

The mainland territory of Ecuador (except for the Galápagos Islands), has three clearly distinct geographic regions (Fig. 1):

1. La Costa, the coastal region located westwards of the Andes and reaching the westernmost point of Santa Elena. This is a most fertile agricultural region of the country, important for food production (bananas, rice, fisheries) and notable for largely populated cities, including Guayaquil.
2. The Andes is the central part of the country, which encompasses Andean highlands. This is a seismically active region where volcanism and repetitive

earthquakes of various magnitude are often recorded. The capital Quito and some other importance cities are located in the Sierra of Andes, e.g. Cuenca.

3. The Amazonia, a scarcely populated region covered by the Amazon jungle rainforests and National Parks with existing geological exploration activities in the forests. The rivers here form a dense tributary network of the Amazon and include, among others, the Napo, Aguarico and Coca rivers.

The geographically distinct regions of Ecuador are formed under the strong influence of geologic setting that largely affected their formation in the geologic past (Fig. 2). While the largest notable areas in the country are notable for Triassic (T) outcrops, the full list of formations include the Precambrian–Devonian (AD), Cretaceous–Tertiary volcanics (Cv), Jurassic (J), Cretaceous (K), Mesozoic–Cenozoic intrusives (MCi), Mesozoic volcanics (Mv), Precambrian undifferentiated (pC),

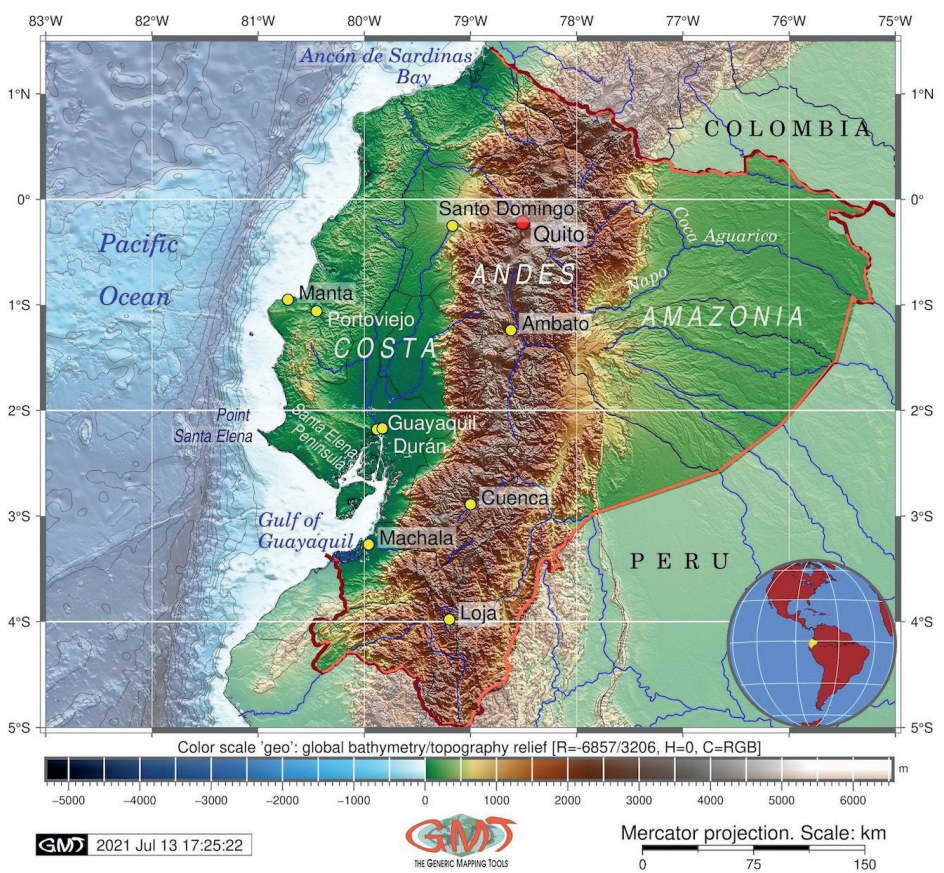

Fig. 1 – Ecuador: Topographic map. SRTM/GEBCO 15 arc second resolution terrain model grid, 2021.

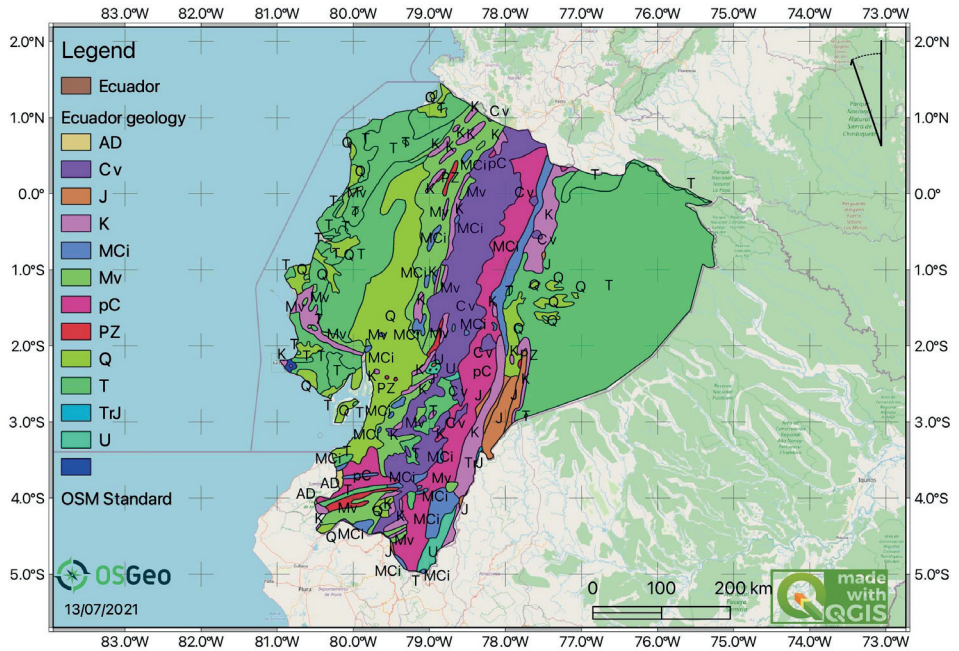

Fig. 2 – Ecuador: Geologic map (QGIS 2021)

Paleozoic (PZ), Quaternary (Q), Triassic (T) and Triassic–Jurassic (TrJ). Here the 'no data' areas are classified as unmapped and noted as 'U', while water lake areas are colored dark blue (Fig. 2). The geology of Ecuador shows the geologic province map of the country as an area clipped from the continent of South America. Mapping was done using vector data from the U.S. Geological Survey (Schenk, Viger, Anderson 1998) selected using the Digital Chart of the World (DCW) for Ecuador.

The country can be divided into the five litho-tectonic divisions, which reflect the fundamentally important events in the tectonic evolution of the Northern Andes since Mesozoic, e.g. dextral transpression of the Andes. The important milestones of the early geologic history in modern Ecuador are summarized as follows. The oldest event recognized during the break-up of western Gondwana related to the Late Triassic age is the intrusion of calc-alkaline batholiths in Jurassic followed by the accretion of the volcano-sedimentary terrane, of oceanic or marginal basin origin, and gneissic Chaucha-Arenillas terrane, to continental South America in Jurassic to Early Cretaceous (Aspden, Litherland 1992).

Detailed paleogeographic evolution of the Ecuadorian foreland is based on the multi-source data from the stratigraphic, sedimentologic and geochronological analysis, depositional ages and sediment dispersal patterns. These data enabled

to reconstruct the geologic history of Ecuador in the Mesozoic-Cenozoic time. Specifically, the retroarc Amazon region of Ecuador recorded distinct events preserved in the Mesozoic-Cenozoic sedimentary record of the Subandean Zone and Oriente Basin. During the Early Jurassic, marine deposits of the Santiago Formation formed a carbonate platform in eastern Ecuador. At about 180 Ma, an eastward-prograding deltaic system transported volcaniclastic material from the western volcanic arc. The nonmarine conditions prevailed during most of the Jurassic, characterized by the deposition of the red beds and volcanic and volcaniclastic deposits of the Chapiza Formation. Clastic and volcanic deposition from ~160 to 130 Ma was coeval with regional extension (Vallejo et al. 2021).

Separated from the main region by geomorphic landforms, the Cordillera Real and sub-Andean Zone of Ecuador are less studied with very little detailed mapping and age control (Pratt, Duque, Ponce 2005), while this region is important for seismic and tectonic setting of the country.

This region is composed of Triassic and Jurassic plutons emplaced into Palaeozoic and metamorphosed volcanic rocks (Fig. 2). Regional variations in geologic history and geodynamic evolution are mirrored in the geomorphic structure of the Earth's landforms and inherited in local topographically irregularities (Hernández et al. 2020; Lemenkova 2020c, 2021b, 2021d). Thus, central and northern parts of the Cordillera Occidental of the Andes of Ecuador comprise two terranes. The Pallatanga terrane consists of the Cretaceous oceanic plateau suite, late Cretaceous marine turbidites of basaltic to andesitic volcanic source, and a tectonic mélange of late Cretaceous age. The Macuchi terrane consists of basaltic to andesitic sources, accreted to the Pallatanga terrane during the Eocene along the Andean margin (Hughes, Pilatasig 2002).

The Eocene and Late Cretaceous periods are notable for the sediment deposition (Álava, Jaillard 2005) with clastic deposits of the Western Cordillera. This area experienced accretion of the oceanic terranes form Western Cordillera and Coast of Ecuador. The mineral and petrographic content of the underlying rocks in Ecuador were formed as a result of the tectonic evolution which evolved in a backarc during the Ordovician and Carboniferous periods (Spikings et al. 2021).

The magmatism associated with tectonic activity and seismicity is caused by the intrusion during the Late Oligocene–Early Miocene period. This time is important for understanding geologic evolution of Ecuador, as the distribution of Tertiary Ecuadorian arc magmatism was dated in Late Oligocene–Early Miocene arc and resulted in magmatic events and eruptions (Schütte, Chiaradia, Beate 2010). Coastal Ecuador is made up of an oceanic igneous basement overlain by Upper Cretaceous to Lower Paleocene (≈98–60 Ma) volcanic rocks of island-arc origin. The igneous basement, known as the Piñón Formation, dated at 123 Ma, consists of basalts and dolerites. The basement of coastal Ecuador presents an accreted fragment of an oceanic plateau (Reynaud et al. 1999).

The aspects of the seismic risk are higher for the historical heritage of the ancient pre-Columbian Inca Empire and cultural cities that should be protected, e.g., Ingapirca, Cuenca with its architectural and archeological highlights, the Pumapungo Archaeological Park and Ruins of Todos Los Santos, Pucara de Rumicucho in northern Ecuador. Therefore, monitoring and modelling earthquakes is important for earthquake risk assessment and conservation of archaeological heritage. Spatial parameters of earthquakes include such factors as focal depth, mechanism and the location of the event. Other aspects include tectonic activity, strength of earthquake and attenuation of seismic waves in the Earth's crust.

In seismology, earthquake hazard includes analysis of a danger of the earthquake occurrence from the physical point of view, that is, the tectonic setting, acting stress, rheology of the focal zone and regional geologic setting. Besides, the existing correlation between the strength properties of rocks and soils and ground stability is reported earlier (Baykara et al. 2020; Lemenkov, Lemenkova 2021b, 2021c). The analysis of geologic data is an effective tool for assessment of the probability of earthquakes and their effects of local geologic setting. Therefore, a brief geologic introduction including tectonic history of Ecuador is briefly outlined below. At a national scale, consequences of earthquakes in Ecuador might be serious due to specific natural and social factors. Therefore, earthquake risk should be assessed with regard to social and physical consequences of earthquakes. Social aspects include the evaluation of how dangerous could the earthquake be concerning victims, damages and economic losses, exposure of constructions (buildings, roads, bridges, houses), and vulnerability of people at risk. Physical aspects include expose to earthquakes due to the regional geological and glaciological setting, repetitive volcanic activity (Granados et al. 2021).

The existing studies on the geology of Ecuador describe in details the evolution of the region in context of the early history of the Earth and South American continent. However, they have not so far integrated technical methods of the scripting for cartographic visualization of seismic and geophysical datasets specifically on Ecuador in an integrated study. At the same time, in case of earthquake risk assessment, including the analysis of physical and social consequences, high-quality mapping and analysis of seismic and topographic data is required. Thus, this study aims to fill this gap by presenting the advanced methods of data processing, modelling and visualization as a contribution to the previous works on the geology, geophysics and seismicity of Ecuador (e.g., Lavenu, Winter, Dávila 1995; Dumont et al. 2005; Goretti, Hutt, Hedelund 2017; Pulido, Yoshimoto, Sarabia 2020). This study presents six new maps made using scripting toolset Generic Mapping Tools (GMT). The maps demonstrate the seismic, geophysical and topographic settingin Ecuador using high-resolution actual data.

Specifically, this study presentsscripting approach of cartographic mapping using GMT. Scripting cartography is a novel method of spatial data analysis and

visualization. It uses syntax of language with predefined commands for writing scripts used for mapping. The reported techniques of data analysis and processing by GMT exist in geological literature (Gauger et al. 2007; Lemenkova, 2020d, 2021a). This study applies these methods for thematic mapping Ecuador with the aim to contribute to the seismic hazard risk analysis. The advantages of GMT over conventional GIS consist in the following. The script-based mapping of GMT utilizes the syntax of embedded language, automates workflows, and analyses data using Geospatial Data Abstraction Library (GDAL). Thus, the GMT enables to make maps with minimal human intervention, and maximal speed, aesthetics and accuracy.

2. Methodology

This section is used to describe the technical details of GMT mapping, and the results are presented in the following section where the achieved values of the geophysical and seismic mapping are discussed with information on data distribution and comparing to the topography of Ecuador. Full scripts used for mapping Figures 1, 3, 4, 5 and 6 by GMT are available on the GitHub: https://github.com/paulinelemenkova/Mapping_Ecuador_GMT_Scripts Creating scripts accessible to the researchers with similar tasks as a technical reference has an aim to facilitate mapping workflow by repeatability of scripts and open access to the codes supported by the GitHub network. Practical approach of scripts created for integration of the GMT modules and sharing access to the codes can facilitate writing such or similar scripts in a cartographic work as a practical reference with working GMT syntax. In this way, developing new GMT codes and algorithms of spatial data processing using high-resolution data would be useful for rapid cartographic visualization and mapping in similar topographic and geophysical studies.

Fundamental cartographic theory addressed in this study using scripting techniques accepts that from a practical viewpoint, conceptual mapping workflow is important. The variety of cartographic products include a wide variety of thematic maps that can be classified into analytical, complex and synthetic maps Beránek (1991). Therefore, mapping includes various approaches aimed at specific purposes, as reflected in constant development of cartographic techniques (Beránek 1995; Voženílek 1999; Konečný, Voženílek 1999; Česák, Šobr 2005; Janský et al. 2005; Robinson et al. 2017; Jenny et al. 2021). Mapping affects visual representation of maps as a product used for spatial analysis of geographic phenomena (Zálešáková 1995; Siwek, Kaňok 2000; Sarhadi, Soltani, Modarres 2012; Zou, Wang, Wang 2012). In this way, effective techniques of mapping helps to reveal hidden correlations between spatial phenomena and to highlight variations in geographic data (Arabameri et al. 2019; Hind 2020; Yousefi et al. 2020; Reddy et al. 2022).

The unique feature of cartography consists in its multi-disciplinary character which makes it both a scientific discipline (as a branch of geography), and a practical technology of data processing and visualization as a special art (D'Ignazio 2020; Otto, Gustavsson, Geilhausen 2011). Therefore, various structural approaches of cartographic workflow can be implemented in the process of mapping for technical optimization of process and for improving the design and aesthetics of the final layouts (Eastman 1985; Wesson 2007; Wang, Zhu 2011; Xiao, Armstrong 2012; Kennelly 2015; Griffin et al. 2017). In this study, the scientific content of the main cartographic activities included the following steps:

1. Data capture through semantic web search based on the analysis of metadata and suitability of the collected raw data as the main factors responsible for the final quality of maps: resolution, extent, origin, reliability, actuality, data types and formats.
2. Data management: organizing and storing in a working directory with defined path in the GMT environment.
3. Writing scripts using GMT syntax. Here various modules of GMT were used for cartographic data processing: format conversion, projecting, clipping, interpolation, coloring, plotting, etc.
4. Cartographic implementation and adjusting scripts for data processing after data analysis, and interpretation. This includes defining spatial extent, selecting optimal cartographic projection, analysis of data range by GDAL for choosing the best color palette to highlight data variation.
5. Running scripts from the GMT console for automatic mapping and visualization.
6. Analysis and classification of objects varying in values (e.g., ranging earthquakes by magnitude, bathymetric steps by depth intervals) and visualization of data at pixel level by uniquely assigned to classes of object categories explained the color legends.

Key deliverables achieved in the cartographic scripting process included developed algorithms of mapping and methods of spatial data processing, applied for both data types (raster images and vector objects). Furthermore, the tasks of cartographic design were adjusted flexibly for various maps depending on the examined data (e.g., is it a visualization of seismicity based on tabular data from IRIS, a geoid model, or a topographic map).

The spatial extent of the study area extends from the southern border of Ecuador with Peru (5°S) to its northern border of Ecuador with Colombia (1.5°N), and stretches longitudinally between the 83°W and 75°W. The elevation data range from minimum of –5,319 m in the Peru-Chile Trench, to the maximum at 6,560 m in the Andes.

The technical aim of the study consists in plotting of six maps using GMT (Wessel et al. 2019) and QGIS (QGIS.org 2021) to compensate for the lack of the

existing seismic maps of Ecuador in topographic and geophysical context using scripting. In this way, this study presents maps of geophysical, seismic and topographic setting of Ecuador by integrating high-resolution data on seismic events and visualizing variability of the topographic and gravimetric structures. The data were collected from the available open sources: Earth Gravitational Model 2008 EGM-2008 (Pavlis et al. 2012) for geoid, General Bathymetric Chart of the Oceans (GEBCO; Schenke 2016) and Shuttle Radar Topography Mission (SRTM) for topography and coastal bathymetry (Farr et al. 2007), Scripps Institution of Oceanography (SIO) data on gravity (Sandwell et al. 2014) and Incorporated Research Institutions for Seismology (IRIS; Iris Transportable Array 2003) for seismicity.

The applications of the conventional Geographic Information system (GIS) are useful in data visualization based on the vector layers (Villacreses et al. 2017, Bydekerke et al. 1998, Klaučo et al. 2013, Lemenkova 2021c). However, they do not allow speed and accurate data processingwhen the amount of datasets require script-based applications and automated data processing. In contrast to the traditional GIS, GMT easily operates with spatial data formats and specifications and enables more effective data processing. Its major technique is based on scripts that enable to import raw datasets in various formats including IRIS seismic tables and to compile layouts in PostScript format, flexibly transformable to the existing graphical standard formats, such as JPG or TIFF with user-defined resolution (e.g., 300 or 720 dpi).

The GMT embeds the variety of map symbols that can be changed and adjusted in an automated way. For instance, the display scale and the projection are smoothly adjustable in GMT using the '-J' function (e.g. -JM6.5i for the 6.5-inch map in Mercator projection). Several GMT modules were used to generate presented maps in Figures 1, 3–6 for Ecuador. For each line of the code, the corresponding GMT module was applied for visualization of the respective elements. The modules grdimage, grdcontour, psscale, psbasemap, psxy, pslegend, psconvert, psxy were considered.

In GMT, we used scripting algorithms for semi-automated mapping by several approaches: The 'grdcut' module for shortening the layer to the size of the area of interest based spatial extent. Raster layer cropping was made using the 'grdcut' module for clipping the data with global coverage, e.g., the country of Ecuador selected from the global topographic grid. Thus, to visualize the topographic map of Ecuador (Fig. 1), the data from the GEBCO grid were used in netCDF format selected for the range of study area as follows: 'gmt grdcut GEBCO_2019.nc -R277/285/–5/1.5 -Gec_relief.nc'.

Script-based mapping of GMT enables to accurately visualise segments of topographic range by adjusted coloring of the palettes that represent the major steps in topographic elevations by 500 meters (Fig. 1). Besides, GMT enables to

semi-automatically map the standard cartographic elements (scale, title, subtitles, annotations, legend, insert globe map) and adjust graphic representation of the geographic meridians and parallels by selecting proper step for cartographic grid and graticule ticks. The isolines were plotted using the ETOPO1 data covering the extent of the digital map of topographic elevation and bathymetric depths acquired from the NOAA. Generating contours for topographic maps from digital elevation models (DEMs) is a common task in geoinformation and cartography discussed in previous papers (Kettunen, Koski, Oksanen 2017; Raposo 2020). In this work, contour lines were depicted using the following code: 'gmt grdcontour ec_relief1.nc -R -J -C500 -W0.1p -O -K >> $ps'. The texts with corresponding cities were then added at corresponding locations using decimal degrees of the map: 'gmt pstext -R -J -N -O -K \ -F+f10p,0,white+jLB+a-0 >> $ps << EOF 280.22–2.18 Guayaquil EOF'. The topographic data range was inspected using GDAL as follows: 'gdalinfo ec_relief.nc -stats' and the following data were received: minimum = –5,319 m, maximum = 6,560 m. These values were used for generating the color palette according to the data extent.

The Quantum GIS (QGIS) was applied for visualization, classification and analysis of geological maps using open data in vector format. We have differentiated classes of various categories of geologic layers and types of outcrops and clipped the area covering Ecuador from the South America overlaied the geologic layer over the OpenStreetMap layer (OSM), Figure 2. The classes have been extracted from the vector data of geologic provinces by the Digital Chart of the World (DCW) layer and visualized into geologic categories using the functionality of QGIS. The QGIS is a traditional GIS software for geoinformation and geospatial data analysis and mapping. Thus, Figure 2 shows the geologic setting of the country. It was plotted using the combination of the USGS geologic data, available for the South America, the OSGeo OpenStreetMap basis layer and the DCW layer with country codes enabling to clip the Ecuador from the surrounding countries. The data were imported to the QGIS project in.shp and raster formats and visualized using the standard GUI interface of the QGIS.

For seismic map (Fig. 3), the lines of the fracture zones were plotted using the 'psxy' module: 'gmt psxy -R -J GSFML_SF_FZ_RM.gmt -Wthicker,pink -O -K >> $ps'. The earthquakes were visualised using the code line 'gmt psxy -R -J quakes_EC.ngdc -Wfaint -i4,3,6,6s0.06 -h3 -Scc -Csteps.cpt -O -K >> $ps'. Specifically, in this code the '-i4,3,6,6s0.06' corresponds to the number of columns showing the coordinates, magnitude and depths of the events, and the 'quakes_EC.ngdc' is the name of the table converted from the CSV format that was downloaded from the IRIS site (Fig. 3). The colors of the earthquakes points correspond to their magnitude as explained in the legend. The identification of the spatial extent of topography was performed using the data range by GDAL (gdalinfo) and correspondingly adjusted color palette.

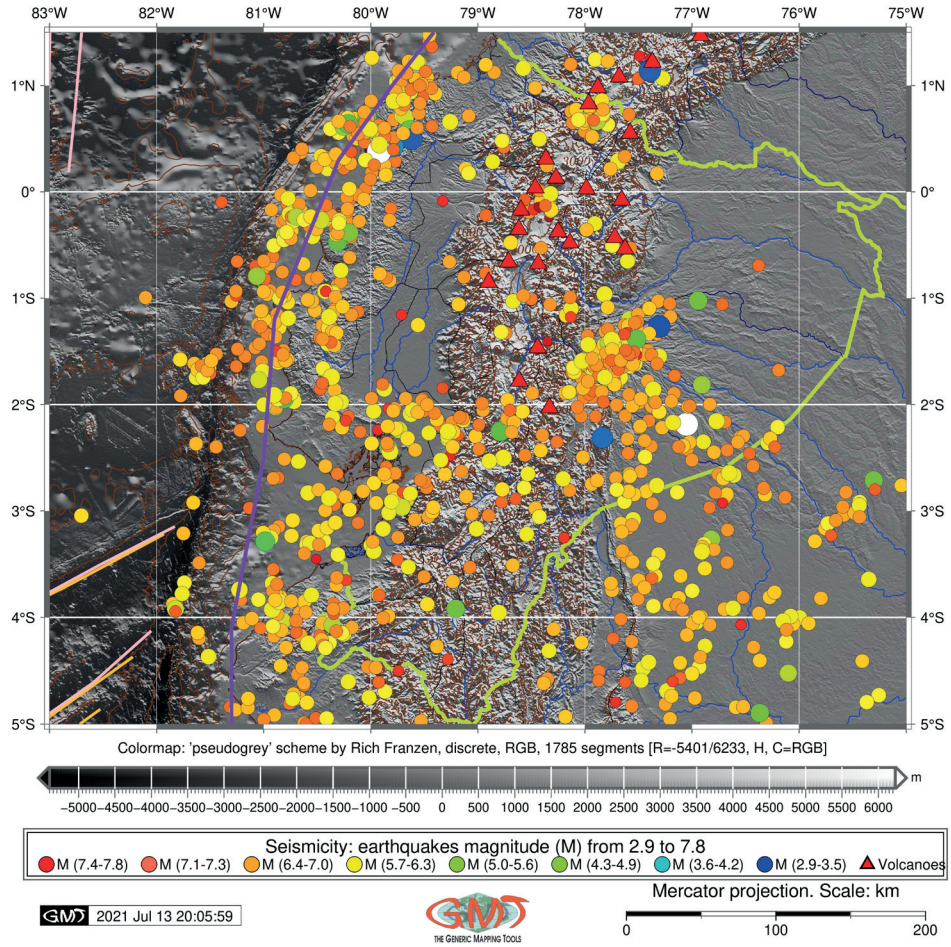

Fig. 3 – Ecuador: Seismic map. Base DEM map: SRTM/GEBCO, 15 arc second resolution. Earthquakes: IRIS Seismic Event Database (2005–2021).

For geoid mapping (Fig. 4), the EGM-2008 data from the National Geospatial-Intelligence Agency (NGA) EGM Development Team covering and adjacent to Ecuador were downloaded. Because the original data were in the ADF format (w001001.adf) the data were converted respectively using the 'grdconvert' GMT module: 'gmt grdconvert s45w90/w001001.adf geoid_01.grd' and 'gmt grdconvert n00w90/w001001.adf geoid_02.grd'. Variations in geoid undulation were visualized using 'grdimage' module by merging two neighbor tiles of the original grid and automatically located by coordinates of the tile's borders within the image extent. The resulting data were inspected using the GDAL: 'gdalinfo geoid_01.grd -stats' and the following outcomes were received: minimum = –28.476,

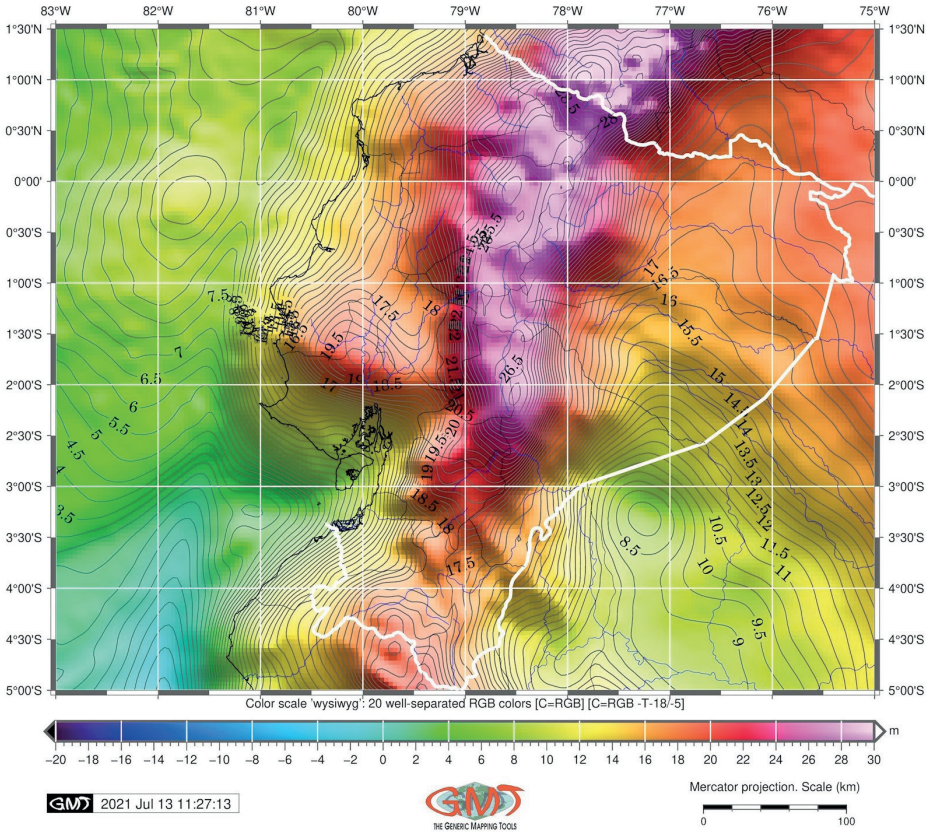

Fig. 4 – Ecuador: Geoid map. Data: World geoid EGM-2008 vertical datum 2.5minute resolution.

maximum = 50.095, which shows the values of geoid over the Ecuador and its surroundings. The cartographic grid was visualized using module 'psbasemap' for a regular grid and annotations for readability of map, extracted geoid tiles from the EGM-2008 colored using the 'wysiwyg' color palette. The analysis of data shows higher values over the region of the Andes (bright magenta colors in Fig. 4) with the lower values over the water areas of the Pacific Ocean.

Satellite-derived data acquisition provided large resolution images of gravity acquired from satellite altimetry Cryo-Sat-2 and Jason-1 (Sandwell et al. 2014). These data were used for gravimetric mapping (Fig. 5 and 6). Figures 5 and 6 show mapped free-air gravity raster grids available online from the UC San Diego, Scripps Institution of Oceanography (SIO). The advantages of the remote sensing (RS) data in mapping consists in high reliability of the data sources, since satellites operate autonomously and provide data as parallel flight stripes along the route of the satellite. As a result, the survey results in a global coverage of the Earth's

gravimetry with certain overlaps (side and forward stripes, depending on technical characteristics of the satellites). These data were used to identify and visualise the anomalies and the variations in the Earth's gravity in acceleration (mGal), along with vertical gravity data (Figures 5 and 6).

For mapping the two grids the following GMT modules were applied: gmtset, gmtdefaults, img2grd, makecpt, grdimage, psscale, grdcontour, psbasemap, gmtlogo, psconvert, pscoast. The grid was first clipped for the region of study area as follows: 'gmt img2grd grav_27.1.img -R277/285/–5/1.5 -Ggrav_EC.grd -T1 -I1 -E -S0.1 -V'. Here the 'img2grd' module of GMT performs the conversion of raster data in IMG format into the GRD format and the '-R277/285/–5/1.5' corresponds to the selected study area with 0–360° convention for the western hemisphere. The data

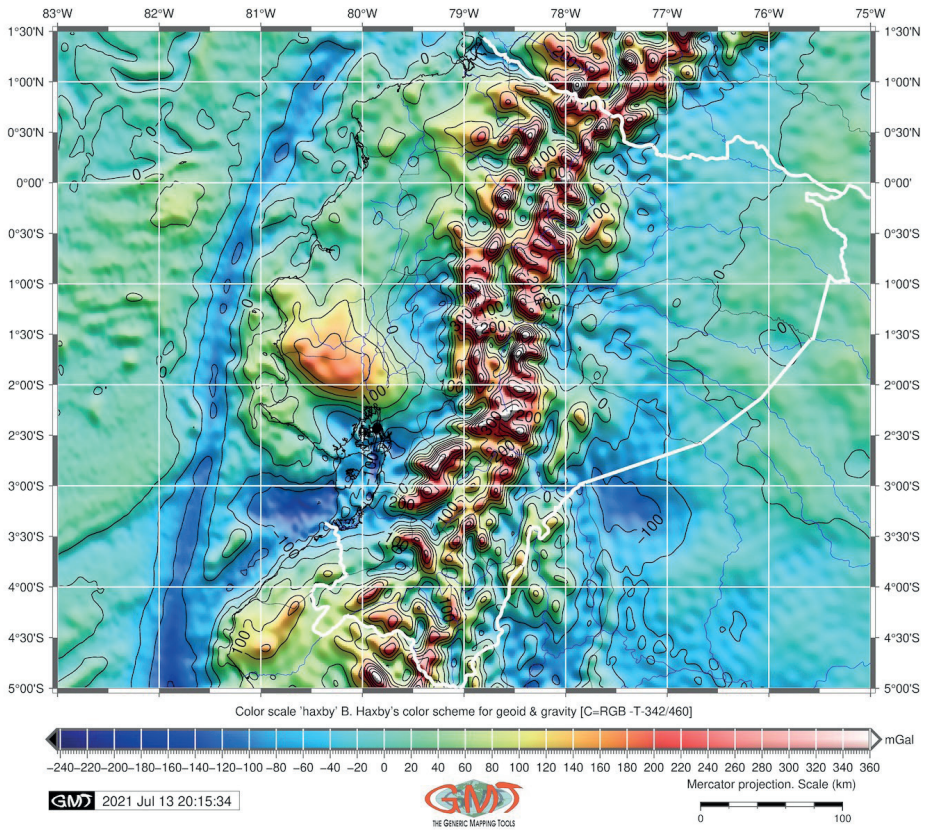

Fig. 5 – Ecuador: Free-air gravity anomaly map. Data source: remote sensing Earth observations of gravity grid from CryoSat-2 and Jason-1, 1 minute resolution, Scripps Institution of Oceanography (SIO), National Oceanic and Atmospheric Administration (NOAA), National Geospatial-Intelligence Agency (NGA).

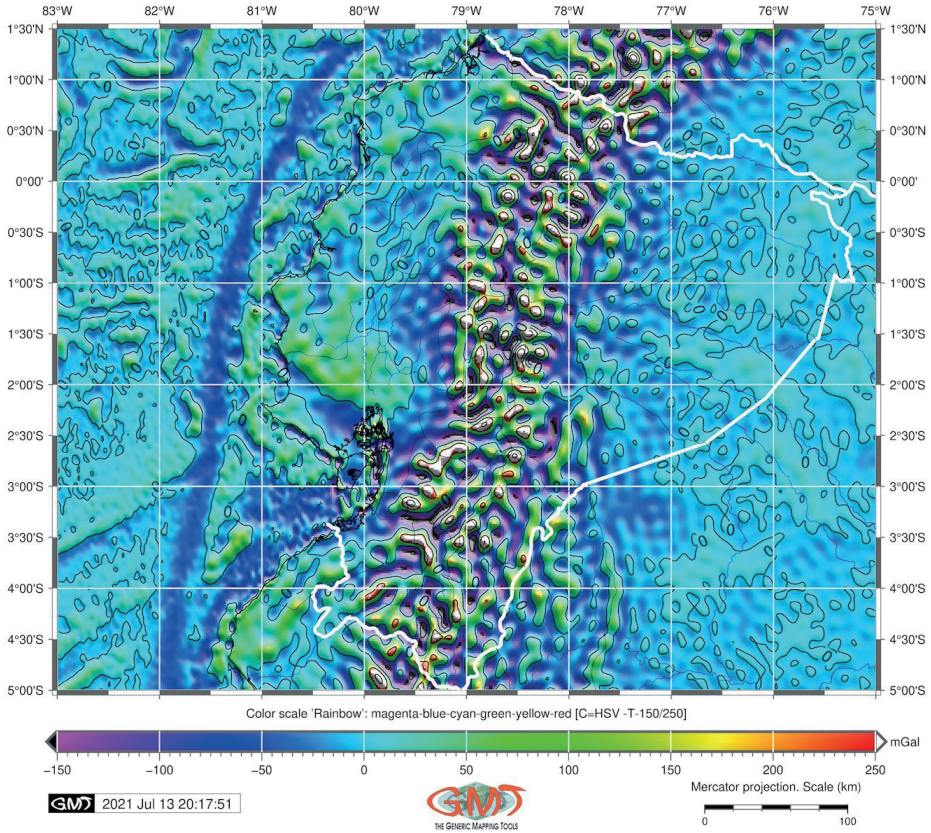

Fig. 6 – Ecuador: Vertical free-air gravity anomaly map. Data source: remote sensing Earth observations of gravity grid from CryoSat-2 and Jason-1, 1 minute resolution, Scripps Institution of Oceanography (SIO), National Oceanic and Atmospheric Administration (NOAA), National Geospatial-Intelligence Agency (NGA).

were inspected for the range and selected color palette was applied as follows: 'gmt makecpt -Crainbow -T-150/250 > colors.cpt' (Fig. 6). The georeferencing of the raw RS data is performed automatically based on the GPS trajectories during the flights of the satellite. The re-projecting into specific projections is possible in GMT using the 'grdimage' module. In this case, we used function '-JM6.5i', which signifies the Mercator projection with 6.5 inches of the geometric extent of the map.

The plausible data covering Ecuador and surrounding areas were visualized using the adjusted color palette corresponding the data range. These data allowed raster grid to be mapped using the following code: 'gmt grdimage grav_EC.grd -Ccolors.cpt -R277/285/−5/1.5 -JM6.5i -P -I+a15+ne0.75 -Xc -K > $ps' (Figure 5). The isolines were plotted using the 'grdcontour' GMT code by the following example

(snippet for Fig. 5): 'gmt grdcontour grav_EC.grd -R -J -C50 -A100 -Wthinner -O -K >> $ps'. The legends were mapped using 'psscale' with defined aesthetic elements and precise location of the legend as follows: 'gmt psscale -Dg277/–5.6+w16.5c/0.4c +h+o0.0/0i+ml+e -R -J -Ccolors.cpt -Bg50f5a50+l"Color scale 'Rainbow': magenta-blue-cyan-green-yellow-red [C=HSV -T-150/250]" -I0.2 -By+l"mGal" -O -K >> $ps'. The gravity grids (Figures 5 and 6) captured from satellite data were as a reference dataset for geophysical modelling over Ecuador and cartographic interpretation of the gravity anomaly fields in regional scale supported by topographic data from the SRTM DEM for comparison (Fig. 1).

3. Results and discussion

The challenges of multi-sources data integration and mapping demonstrated in this study respond to the needs of this multi-disciplinary project that combines advanced technologies of cartographic scripting by GMT, conventional GIS techniques by QGIS, high-resolution data and practical applications towards seismic risk assessment in Ecuador through the visualization of earthquake locations and magnitude. Open source high-resolution data used in this study include topographic, geologic and geophysical datasets, data on seismicity and satellite-derived gravity grids. Here the maps are based on the publicly accessible data that can be reused in similar studies. The country-level coverage of Ecuador is presented in all the maps in identical cartographic projection to allow the comparison of maps. While the major instrument of this study is the GMT, the QGIS is used as an additional tool for comparative cartographic technologies.

Figures 1 and 2 show the main topographic and physio geographic regions of the Ecuador and corresponding geologic map with provinces. Figure shows the topographic values of GEBCO/SRTM by elevation steps, along with added contour lines by based on the ETOPO1. Three distinct regions of the landscapes of Ecuador area visualized: the Costa, the Andes and the Amazonia. The Triassic outcrops well corresponds to the Amazonia region of Ecuador, while the Andean geology demonstrate the complexity and mixed layers of the Cretaceous–Tertiary volcanics (Cv), Precambrian (Pc) and Mesozoic–Cenozoic intrusives (MCi) that played the significant role in the geologic evolution and formation of Ecuador, as mentioned briefly in the Introduction section of this document.

Figure 3 shows the values of seismic events that were analyzed based on the IRIS database. The table from among the 1,000 total values of events was studied. The depth of the earthquakes ranges from 0 to 248.3 km (off the coasts of Ecuador, 30 January, 2005). The magnitude ranges from 2,9 to the maximal of 7,8 (27 km SSE of Muisne, April 16, 2016 at depth of 20.6 km). Another notable seismic event with magnitude over 7.0 is recorded in the 111 km ESE of Palora (magnitude = 7.5,

depth = 145 (April 16, 2016). The comparison of the seismicity map (Fig. 3) with topographic elevations (Fig. 1) shows the three major areas of seismically active zones in Ecuador: (1) the Andes region that well corresponds to the tectonically active mountains; (2) the coastal submarine earthquakes that are concentrated along the Peru-Chile Trench; (3) the easter Cordillera region that is located to the east of Andes and overlaps the Peruvian Andes.

Figure 4 shows the intensity of geoid undulations which is visualized using the 'wysiwyg' color palette of GMT and controred by isolines placed every 0.5 m based on the geopotential model of EGM-2008 data. Comparison of the geoid heights (Fig. 4) with the high-resolution digital terrain model (GEBOC/SRTM) shows remarkable correlations between the geodetic values and the regional topography of Ecuador. Namely, the values of geoid are the most prominent throughout the extent of the Andes (bright pink colors in Fig. 4) with the maximal values reaching 25.5 m, which well corresponds to the increased gravity values and stronger land masses in the mountains, while the lower values are mostly elongated well depicting the Peru-Chile Trench with values from –2.0 to 8.5 (cyan colors in Fig. 4). Thus, the gravimetric geoid determination corresponds with the gridded terrain, geometry of the geomorphological contours (e.g. the extent of the Andes), topographic density of landmasses with highly heterogeneities patterns and land mass deficit in the oceanic trench and the increase of land masses in high mountain region.

Figures 5 and 6 show the values of the gravity observations and vertical gradient based on the open access geophysical data from the SIO. The data show the remarkable correlation with the higher values in the Andes (over 200 mGal, red areas in the Figure 5) and clearly distinct low values that correspond to the Peru-Chile Trench and the Gulf of Guayaquil (< –100 mGal, dark blue colors in Fig. 5). Small yet notable increase in values is visible north of the Santa Elena Peninsula in the local mountain range that can also be compared with topographic map in Figure 1. In the west, along the coasts of the country, the Peru-Chile Trench is depicted in Figure 6 as the lowest values in vertical gravity that shows gradient of variations.

4. Final conclusions

The Geographic Information Systems (GIS) have been widely used for geoscience since about 1980s and their applications are being constantly increasing along with rapid computerization of methods. The need for effective visualization of datasets and availability of open source data raised the variety of GIS that has been used in various domains of Earth sciences, such as marine geology, environment and ecology, urban studies, geographic analysis, seismic, geological and geophysical studies (Hoskins et al. 2021; Lemenkova 2022; Soriano et al. 2017;

Klaučo et al. 2017; Gouvea, Nucci, Liberti 2021; Suetova, Ushakova, Lemenkova 2005; Lindh, Lemenkova 2021a, 2021b; Cabral, Neto 2020; Schenke, Lemenkova 2008). In contrast to the traditional GIS, the demonstrated the scripting approach actively uses automatization in cartographic data processing and adjusted graphical design which resulted in effective workflow and accurate maps of seismicity, topographic and geophysical setting of Ecuador.

A key to the automatization in production of cartographic displays is console-based scripting which can be done using GMT. Scripting operates in an approach similar to the programming or markup languages (Lemenkov, Lemenkova 2021a) by using a certain syntax of the code used for generating scripts that can be run from the console for plotting maps. Among the most reputable cartographic tools are the GRASS GIS and the GMT (Lemenkova 2019b, 2020b). The GMT demonstrated in this study brings evident benefits to seismic and geophysical mapping through the automated workflow and accurate data handling. Using the case study of Ecuador, this research presented several maps made using GMT and one map using the QGIS and plugins for OSGeo. The results show topographic, geophysical, seismic and geologic visualization of Ecuador. The presented series of maps demonstrated correlations between the tectonic and geological phenomena reflected in the topographic elevations of the country. Besides, the geophysical data aimed for digital seismic monitoring of Ecuador will allow to gain new knowledge through the analysis of maps and the reuse of maps. The provided GitHub link with open access codes brings new opportunities to cartographers through the easy access to shared repository with MT scripts for repeatability.

The presented series of geophysical and seismic maps of Ecuador is a set of new six machine-based cartographic outputs. The data for seismicity are based on the IRIS catalogue by the Bulletin of the International Seismological Centre (ISC). The maps are totally different of the traditional handmade maps that are made using conventional Graphical User Interface (GUI) in GIS. The presented maps of Ecuador are made using the machine graphics of GMT scripts from the console and computer-generated plots. As a result, the outputs present refined aesthetic maps with optimized design approaches. In contrast to the traditional GIS, using GMT scripting toolset enables to balance and improve usual monotonous cartographic workload of mapping by presenting a variety of optimal decisions and refined solutions regarding mapping process.

Scripting cartography is currently the fastest growing discipline in geoinformatics. Using diversified multi-format open source data, scripting cartography enables not only the conventional mapping but also to perform image processing using R language for spatial data analysis. Scripting cartographic techniques demonstrated in this study can be applied not only in geologic and geophysical mapping but also in a wide variety of Earth sciences domains, such as environmental and ecological analysis, hydrologic riverine and lacustrine modelling, ocean and

polar research, urban sprawl, land cover and use detection by image processing based on the remote sensing data, to mention a few.

The main disadvantage associated with the use of traditional GIS methods consists in the amount of human-operated actions of preparing various elements of map layout. Because human-based data processing can be prone to errors, accidental mistakes and misleading visualization, using scripts is the effective alternative in cartography to the traditional GIS. To this end, a script-based approach byGMT is applied in this study for mapping Ecuador. Thus, the study demonstrated a series of maps made using scripting from a console that enables to smoothly process and integrate seismic, geophysical and topographic multi-format data. Such an approach is especially advantageous for seismic risk mapping and hazard assessment in tectonically active regions of Ecuador, because it enables rapid machine-based mapping in real time regime.

References

AGURTO-DETZEL, H., FONT, Y., CHARVIS, P., RÉGNIER, M., RIETBROCK, A., AMBROIS, D., PAULATTO, M., ALVARADO, A., BECK, S., COURBOULEX, F., DE BARROS, L., DESCHAMPS, A., HERNANDEZ, M.J., HERNANDEZ, S., HOSKINS, M., LEÓN-RÍOS, S., LYNNER, C., MELTZER, A., MERCERAT, E.D., MICHAUD, F., NOCQUET, J.M., ROLANDONE, F., RUIZ, M., SOTO-CORDERO, L. (2019): Ridge subduction and after slip control aftershock distribution of the 2016 Mw 7.8 Ecuador earthquake. Earth and Planetary Science Letters, 520, 63–76.

AKHOONDZADEH, M., DE SANTIS, A., MARCHETTI, D., PISCINI, A., CIANCHINI, G. (2018): Multi precursors analysis associated with the powerful Ecuador (MW=7.8) earthquake of 16 April 2016 using Swarm satellites data in conjunction with other multi-platform satellite and ground data. Advances in Space Research, 61, 1, 248–263.

ALVARADO, A., RUIZ, M., MOTHES, P., YEPES, H., SEGOVIA, M., VACA, M., RAMOS, C., ENRÍQUEZ, W., PONCE, G., JARRÍN, P., AGUILAR, J., ACERO, W., VACA, S., SINGAUCHO, J.C., PACHECO, D., CÓRDOVA, A. (2018): Seismic, volcanic, and geodetic networks in Ecuador: building capacity for monitoring and research. Seismological Research Letters, 89, 432–439.

ÁLAVA, J.T., JAILLARD, E. (2005): Provenance of the Upper Cretaceous to upper Eocene clastic sediments of the Western Cordillera of Ecuador: Geodynamic implications. Tectonophysics, 399, 1–4, 279–292.

ÁLVAREZ, O., FOLGUERA, A., GIMENEZ, M. (2017): Rupture area analysis of the Ecuador (Musine) Mw = 7.8 thrust earthquake on April 16, 2016, using GOCE derived gradients. Geodesy and Geodynamics, 8, 1, 49–58.

ARABAMERI, A., PRADHAN, B., REZAEID, K., CONOSCENTI, C. (2019): Gully erosion susceptibility mapping using GIS-based multi-criteria decision analysis techniques. CATENA, 180, 282–297.

ASPDEN, J.A., LITHERLAND, M. (1992): The geology and Mesozoic collisional history of the Cordillera Real, Ecuador. Tectonophysics, 205, 1–3, 187–204.

BAYKARA, H., CORNEJO, M.H., ESPINOZA, A., GARCÍA, E., ULLOA, N. (2020): Preparation, characterization, and evaluation of compressive strength of polypropylene fiber reinforced geopolymer mortars. Heliyon, 6, 4, e03755.

BEAUVAL, C., MARINIÈRE, J., YEPES, H., AUDIN, L., NOCQUET, J.M., ALVARADO, A., BAIZE, S., AGUILAR, J., SINGAUCHO, J.C., JOMARD, H. (2018): A new seismic hazard model for Ecuador Bull. Bulletin of the Seismological Society of America, 108, 1443–1464.

BERÁNEK, T. (1991): Cartographic Synthesis and Synthetic Map. Geografie, 96, 3, 177–183.

BERÁNEK, T. (1995): Expert Systems and Their Cartographic Applications. Geografie, 100, 1, 35–41.

BYDEKERKE, L., VAN RANST, E., VANMECHELEN, L., GROENEMANS, R. (1998): Land suitability assessment for cherimoya in southern Ecuador using expert knowledge and GIS. Agriculture, Ecosystems & Environment, 69, 2, 89–98.

CABRAL, A.E., NETO, R.M. (2020): Mapeamento geomorfológico do município de Campos, Gerais, Sul de Minas Gerais. Caminhos de Geografia, 21, 76, 42–56.

CEVALLOS-MERKI, L., JOERIN, J. (2021): Chapter 11 – Social capital in disaster recovery: A case study after the 2016 earthquake in Ecuador. In: Mendes, J.M., Kalonji, G., Jigyasu, R., Chang-Richards, A. (eds.): Strengthening Disaster Risk Governance to Manage Disaster Risk, Elsevier, 107–115.

ČESÁK, J., ŠOBR, M. (2005): Methods of bathymetric mapping of Czech lakes. Geografie, 110, 3, 141–151.

D'IGNAZIO, C. (2020): Art and Cartography. International Encyclopedia of Human Geography (Second Edition), 189–207.

DUMONT, J.F., SANTANA, E., VILEMA, W., PEDOJA, K., ORDÓÑEZ, M., CRUZ, M., JIMÉNEZ, N., ZAMBRANO, I. (2005): Morphological and microtectonic analysis of Quaternary deformation from Puná and Santa Clara Islands, Gulf of Guayaquil, Ecuador (South America). Tectonophysics, 399, 1–4, 331–350.

EASTMAN, J.R. (1985): Cognitive Models and Cartographic Design Research, The Cartographic Journal, 22, 2, 95–101.

EBMEIER, S.K., ELLIOTT, J.R., NOCQUET, J.-M., BIGGS, J., MOTHES, P., JARRÍN, P., YÉPEZ, M., AGUAIZA, S., LUNDGREN, P., SAMSONOV, S.V. (2016): Shallow earthquake inhibits unrest near Chiles–Cerro Negro volcanoes, Ecuador–Colombian border. Earth and Planetary Science Letters, 450, 283–291.

FARR, T.G., ROSEN, P.A., CARO, E., CRIPPEN, R., DUREN, R., HENSLEY, S., KOBRICK, M., PALLER, M., RODRIGUEZ, E., ROTH, L., SEAL, D., SHAFFER, S., SHIMADA, J., UMLAND, J., WERNER, M., OSKIN, M., BURBANK, D., ALSDORF, D. (2007): The Shuttle Radar Topography Mission. Reviews of Geophysics, 45, 2, RG2004.

FONT, Y., SEGOVIA, M., VACA, S., THEUNISSEN, T. (2013): Seismicity patterns along the Ecuadorian subduction zone: new constraints from earthquake location in a 3-D a priori velocity model. Geophysical Journal International, 193, 1, 263–286.

GAUGER, S., KUHN, G., GOHL, K., FEIGL, T., LEMENKOVA, P., HILLENBRAND, C. (2007): Swath-bathymetric mapping. Reports on Polar and Marine Research, 557, 38–45.

GORETTI, A., HUTT, C.M., HEDELUND, L. (2017): Post-earthquake safety evaluation of buildings in Portoviejo, Manabí province, following the Mw7.8 Ecuador earthquake of April 16, 2016. International Journal of Disaster Risk Reduction, 24, 271–283.

GOUVEA, G.M., NUCCI, J.C., LIBERTI, E. (2021): Cobertura da terra e qualidade ambiental da bacia hidrográfica do Córrego Vila Pinheiros, Curitiba, Paraná (Brasil). Caminhos de Geografia, 22, 80, 153–168.

GRANADOS, H.D., MIRANDA, P.J., NÚÑEZ, G.C., ALZATE, B.P., MOTHES, P., ROA, H.M., CORREA, B.E.C., RAMOS, J.C. (2021): Chapter 17 – Hazards at ice-clad volcanoes: Phenomena, processes, and examples from Mexico, Colombia, Ecuador, and Chile, Editor(s): Wilfried Haeberli, Colin Whiteman, Snow and Ice-Related Hazards, Risks, and Disasters (Second Edition), Elsevier, 597–639.

GRIFFIN, A.L., WHITE, T., FISH, C., TOMIO, B., HUANG, H., SLUTER, C.R., BRAVO, J.V.M., FABRIKANT, S.I., BLEISCH, S., YAMADA, M., PICANÇO, P. (2017): Designing across map use contexts: a research agenda. International Journal of Cartography, 3, 1, 90–114.

HERNÁNDEZ, M.J., MICHAUD, F., COLLOT, J.-Y., PROUST, J.-N., D'ACREMONT, E. (2020): Evolution of the Ecuador offshore nonaccretionary-type forearc basin and margin segmentation. Tectonophysics, 781, 228374.

HIND, S. (2020): Between capture and addition: The ontogenesis of cartographic calculation. Political Geography, 78, 102147.

HOSKINS, M.C., MELTZER, A., FONT, Y., AGURTO-DETZEL, H., VACA, S., ROLANDONE, F., NOCQUET, J.-M., SOTO-CORDERO, L., STACHNIK, J.C., BECK, S., LYNNER, C., RUIZ, M., ALVARADO, A., HERNANDEZ, S., CHARVIS, P., REGNIER, M., LEON-RIOS, S., RIETBROCK, A. (2021): Triggered crustal earthquake swarm across subduction segment boundary after the 2016 Pedernales, Ecuador megathrust earthquake. Earth and Planetary Science Letters, 553, 116620.

HUGHES, R.A., PILATASIG, L.F. (2002): Cretaceous and Tertiary terrane accretion in the Cordillera Occidental of the Andes of Ecuador. Tectonophysics, 345, 1–4, 29–48.

IRIS TRANSPORTABLE ARRAY (2003): USArray Transportable Array. International Federation of Digital Seismograph Networks.

JANSKÝ, B., ŠOBR, M., KOCUM, J., ČESÁK, J. (2005): New bathymetric mapping of the Bohemian Forest glacial lakes. Geografie, 110, 3, 176–187.

JENNY, B., HEITZLER, M., SINGH, D., FARMAKIS-SEREBRYAKOVA, M., LIU, J., HURNI, L. (2021): Cartographic Relief Shading with Neural Networks. IEEE Transactions on Visualization & Computer Graphics, 27, 1225–1235.

JIMÉNEZ, C., SAAVEDRA, M.J., MORENO, N. (2021): Seismic source characteristics of the 2016 Pedernales-Ecuador earthquake (Mw 7.8). Physics of the Earth and Planetary Interiors, 312, 106670.

KENNELLY, P.J. (2015): Complexities of designing terrain maps illustrated with horizontal hachures, International Journal of Cartography, 1, 2, 185–209.

KETTUNEN, P., KOSKI, C., OKSANEN, J. (2017): A design of contour generation for topographic maps with adaptive DEM smoothing, International Journal of Cartography, 3, 1, 19–30.

KONEČNÝ, M., VOŽENÍLEK, V. (1999): Trends in Cartography. Geografie, 104, 4, 221–230.

KLAUČO, M., GREGOROVÁ, B., STANKOV, U., MARKOVIĆ, V., LEMENKOVA, P. (2013): Determination of ecological significance based on geostatistical assessment: a case study from the Slovak Natura 2000 protected area. Open Geosciences, 5, 1, 28–42.

KLAUČO, M., GREGOROVÁ, B., KOLEDA, P., STANKOV, U., MARKOVIĆ, V., LEMENKOVA, P. (2017): Land planning as a support for sustainable development based on tourism: A case study of Slovak Rural Region. Environmental Engineering and Management Journal, 2, 16, 449–458.

LAVENU, A., WINTER, T., DÁVILA, F. (1995): A Pliocene–Quaternary compressional basin in the Interandean Depression, Central Ecuador. Geophysical Journal International, 121, 1, 279–300.

LEGRAND, D., CALAHORRANO, A., GUILLIER, B., RIVERA, L., RUIZ, M., VILLAGÓMEZ, D., YEPES, H. (2002): Stress tensor analysis of the 1998–1999 tectonic swarm of northern Quito related to the volcanic swarm of Guagua Pichincha volcano, Ecuador. Tectonophysics, 344, 1–2, 15–36.

LEMENKOV, V., LEMENKOVA, P. (2021a): Using TeX Markup Language for 3D and 2D Geological Plotting. Foundations of Computing and Decision Sciences, 46, 3, 43–69.

LEMENKOV, V., LEMENKOVA, P. (2021b): Measuring Equivalent Cohesion Ceq of the Frozen Soils by Compression Strength Using Kriolab Equipment. Civil and Environmental Engineering Reports, 31, 2, 63–84.

LEMENKOV, V., LEMENKOVA, P. (2021c): Testing Deformation and Compressive Strength of the Frozen Fine-Grained Soils With Changed Porosity and Density. Journal of Applied Engineering Sciences, 11, 2, 113–120.

LEMENKOVA, P. (2019a): Geomorphological modelling and mapping of the Peru-Chile Trench by GMT. Polish Cartographical Review, 51, 4, 181–194.

LEMENKOVA, P. (2019b): Geophysical Modelling of the Middle America Trench using GMT. Annals of Valahia University of Targoviste. Geographical Series, 19, 2, 73–94.

LEMENKOVA, P. (2020a): Using GMT for 2D and 3D Modeling of the Ryukyu Trench Topography, Pacific Ocean. Miscellanea Geographica, 25, 4, 213–225.

LEMENKOVA, P. (2020b): GRASS GIS for topographic and geophysical mapping of the Peru-Chile Trench. Forum Geografic, 19, 2, 143–157.

LEMENKOVA, P. (2020c): Geomorphology of the Puerto Rico Trench and Cayman Trough in the Context of the Geological Evolution of the Caribbean Sea. Annales Universitatis Mariae Curie-Sklodowska, sectio B – Geographia, Geologia, Mineralogia et Petrographia, 75, 115–141.

LEMENKOVA, P. (2020d): Variations in the bathymetry and bottom morphology of the Izu-Bonin Trench modelled by GMT. Bulletin of Geography. Physical Geography Series, 18, 1, 41–60.

LEMENKOVA, P. (2021a): Topography of the Aleutian Trench south-east off Bowers Ridge, Bering Sea, in the context of the geological development of North Pacific Ocean. Baltica, 34, 1, 27–46.

LEMENKOVA, P. (2021b): Geodynamic setting of Scotia Sea and its effects on geomorphology of South Sandwich Trench, Southern Ocean. Polish Polar Research, 42, 1, 1–23.

LEMENKOVA, P. (2021c): Dataset compilation by GRASS GIS for thematic mapping of Antarctica: Topographic surface, ice thickness, subglacial bed elevation and sediment thickness. Czech Polar Reports 11, 1, 67–85.

LEMENKOVA, P. (2021d): Geophysical Mapping of Ghana Using Advanced Cartographic Tool GMT. Kartografija i Geoinformacije, 20, 36, 16–37.

LEMENKOVA, P. (2021e). The visualization of geophysical and geomorphologic data from the area of Weddell Sea by the Generic Mapping Tools. Studia Quaternaria 38, 1, 19–32.

LEMENKOVA, P. (2022): Console-Based Mapping of Mongolia Using GMT Cartographic Scripting Toolset for Processing TerraClimate Data. Geosciences, 12, 3, 140.

LINDH, P., LEMENKOVA, P. (2021a): Evaluation of Different Binder Combinations of Cement, Slag and CKD for S/S Treatment of TBT Contaminated Sediments. Acta Mechanica et Automatica, 15, 4, 236–248.

LINDH, P., LEMENKOVA, P. (2021b): Resonant Frequency Ultrasonic P-Waves for Evaluating Uniaxial Compressive Strength of the Stabilized Slag–Cement Sediments. Nordic Concrete Research, 65, 2, 39–62.

OTTO, J.-C., GUSTAVSSON, M., GEILHAUSEN, M. (2011): Chapter Nine – Cartography: Design, Symbolisation and Visualisation of Geomorphological Maps. Developments in Earth Surface Processes 15, 253–295.

PAVLIS, N.K., HOLMES, S.A., KENYON, S.C., FACTOR, J.K. (2012): The development and evaluation of the Earth Gravitational Model 2008 (EGM2008). Journal of Geophysical Research, 117, B04406.

PRATT, W.T., DUQUE, P., PONCE, M. (2005): An autochthonous geological model for the eastern Andes of Ecuador, Tectonophysics, 399, 1–4, 251–278.

PULIDO, N., YOSHIMOTO, M., SARABIA, A.M. (2020): Broadband wavelength slip model of the 1906 Ecuador-Colombia megathrust-earthquake based on seismic intensity and tsunami data. Tectonophysics, 774, 228226.

QGIS.org (2021): QGIS Geographic Information System. QGIS Association, http://www.qgis.org.

RAPOSO, P. (2020): Variable DEM generalization using local entropy for terrain representation through scale, International Journal of Cartography, 6, 1, 99–120.

REDDY, Y.S., KUMAR, A., PANDEY, O.J., CENKERAMADDI, L.R. (2022): Spectrum cartography techniques, challenges, opportunities, and applications: A survey. Pervasive and Mobile Computing 79, 101511.

REYNAUD, C., JAILLARD, É., LAPIERRE, H., MAMBERTI, M., MASCLE, G.H. (1999): Oceanic plateau and island arcs of southwestern Ecuador: their place in the geodynamic evolution of northwestern South America. Tectonophysics, 307, 3–4, 235–254.

ROBINSON, A.C., DEMŠAR, U., MOORE, A.B., BUCKLEY, A., JIANG, B., FIELD, K., KRAAK, M.-J., CAMBOIM, S.P., SLUTER, C.R. (2017): Geospatial big data and cartography: research challenges and opportunities for making maps that matter, International Journal of Cartography, 3, 1, 32–60.

SANDWELL, D.T., MÜLLER, R.D., SMITH, W.H.F., GARCIA, E., FRANCIS, R. (2014): New global marine gravity model from CryoSat-2 and Jason-1 reveals buried tectonic structure. Science, 7346, 6205, 65–67.

SARHADI, A., SOLTANI, S., MODARRES, R. (2012): Probabilistic flood inundation mapping of ungauged rivers: Linking GIS techniques and frequency analysis. Journal of Hydrology, 458–459, 21, 68–86.

SCHENK, C.J., VIGER, R.J., ANDERSON, C.P. (1998): Maps showing geology, oil and gas fields, and geologic provinces of the South America region. U.S. Geological Survey Open-File Report 97–470D, 12.

SCHENKE, H. (2016): General Bathymetric Chart of the Oceans (GEBCO). In: Harff, J., Meschede, M., Petersen, S., Thiede, J. (eds): Encyclopedia of Marine Geosciences. Encyclopedia of Earth Sciences Series. Springer, Dordrecht.

SCHENKE, H.W., LEMENKOVA, P. (2008): Zur Frage der Meeresboden-Kartographie: Die Nutzung von AutoTrace Digitizer für die Vektorisierung der Bathymetrischen Daten in der Petschora-See. Hydrographische Nachrichten, 81, 16–21.

SCHUSTER, R.L., NIETO, A.S., O'ROURKE, T.D., CRESPO, E., PLAZA-NIETO, G. (1996): Mass wasting triggered by the 5 March 1987 Ecuador earthquakes. Engineering Geology, 42, 1, 1–23.

SCHÜTTE, P., CHIARADIA, M., BEATE, B. (2010): Geodynamic controls on Tertiary arc magmatism in Ecuador: Constraints from U–Pb zircon geochronology of Oligocene–Miocene intrusions and regional age distribution trends. Tectonophysics, 489, 1–4, 159–176.

SEVILLA, J.H. (1992): Example of big landslides in Ecuador (In French). Proc 6th International Congress International Association of Engineering Geology, Amsterdam, 6–10 August 1990V3,

P1713–1717. Publ Rotterdam: A A Balkema, 1990. International Journal of Rock Mechanics and Mining Sciences & Geomechanics Abstracts, 29, 3, A191.

SIWEK, T., KAŇOK, J. (2000): Mapping Silesian Identity in Czechia. Geografie, 105, 2, 190–200.

SORIANO, G., ESPINOZA, T., VILLANUEVA, R., GONZALEZ, I., MONTERO, A., CORNEJO, M., LOPEZ, K. (2017): Thermal geological model of the city of Guayaquil, Ecuador. Geothermics, 66, 101–109.

SPIKINGS, R., PAUL, A., VALLEJO, C., REYES, P. (2021): Constraints on the ages of the crystalline basement and Palaeozoic cover exposed in the Cordillera real, Ecuador: 40Ar/39Ar analyses and detrital zircon U/Pb geochronology. Gondwana Research, 90, 77–101.

SUETOVA, I.A., USHAKOVA, L.A., LEMENKOVA, P. (2005): Geoinformation mapping of the Barents and Pechora Seas. Geography and Natural Resources, 4, 138–142.

VACA, S., VALLÉE, M., NOCQUET, J.-M., BATTAGLIA, J., RÉGNIER, M. (2018): Recurrent slow slip events as a barrier to the northward rupture propagation of the 2016 Pedernales earthquake (Central Ecuador). Tectonophysics, 724–725, 80–92.

VALLEJO, C., ROMERO, C., HORTON, B.K., SPIKINGS, R.A., GAIBOR, J., WINKLER, W., ESTEBAN, J.J., THOMSEN, T.B., MARIÑO, E. (2021): Jurassic to Early Paleogene sedimentation in the Amazon region of Ecuador: Implications for the paleogeographic evolution of northwestern South America. Global and Planetary Change, 103555.

VILLACRESES, G., GAONA, G., MARTÍNEZ-GÓMEZ, J., JUAN JIJÓN, D. (2017): Wind farms suitability location using geographical information system (GIS), based on multi-criteria decision making (MCDM) methods: The case of continental Ecuador. Renewable Energy, 109, 275–286.

VOŽENÍLEK, V. (1999): Cartographical Tools of Geographical Information Systems. Geografie, 104, 4, 231–242.

WANG, H., ZHU, J. (2011): Interactive Cartographic Drawing within the RIA/Silverlight Environment. in Digital Media and Digital Content Management, Hangzhou, Zhejiang China, 292–297.

WESSEL, P., LUIS, J.F., UIEDA, L., SCHARROO, R., WOBBE, F., SMITH, W.H.F., TIAN, D. (2019): The Generic Mapping Tools version 6. Geochemistry, Geophysics, Geosystems, 20, 5556–5564.

WESSON, C. (2007): Cartographic Design, Quality and Consultancy at Ordnance Survey. The Cartographic Journal, 44, 3, 209–215.

XIAO, N., ARMSTRONG, M.P. (2012): Towards a Multiobjective View of Cartographic Design, Cartography and Geographic Information Science, 39, 2, 76–87.

YAMANAKA, Y., TANIOKA, Y. (2018): Large amplification of the 1906 Colombia–Ecuador earthquake tsunami in Hilo Bay induced by bay-scale resonance. Geophysical Journal International, 214, 3, 1937–1946.

YOUSEFI, S., AVAND, M., YARIYAN, P., POURGHASEMI, H.R., KEESSTRA, S., TAVANGAR, S., TABIBIAN, S. (2020): A novel GIS-based ensemble technique for rangeland downward trend mapping as an ecological indicator change. Ecological Indicators, 117, 106591.

ZÁLEŠÁKOVÁ, D. (1995): Methods of Cartographical Representation of Groundwater Regionalization. Geografie, 100, 1, 10–15.

ZOU, Q., WANG, Q., WANG, C. (2012). Integrated Cartography Technique Based on GIS. Energy Procedia 17, Part A, 663–670.

ACKNOWLEDGEMENTS

The author cordially thanks the two anonymous reviewers and the journal editor for reading, commenting and reviewing the initial version of this manuscript.

ORCID

POLINA LEMENKOVA
https://orcid.org/0000-0002-5759-1089